Controlling the interfacial conductance in $LaAlO_3/SrTiO_3$ in 90° off-axis sputter deposition

Chunhai Yin,[1] Dileep Krishnan,[2] Nicolas Gauquelin,[2] Jo Verbeeck,[2] and Jan Aarts[1]
[1]*Huygens-Kamerlingh Onnes Laboratory, Leiden University, P.O. Box 9504, 2300RA Leiden, The Netherlands*
[2]*EMAT, University of Antwerp, Groenenborgerlaan 171, 2020 Antwerp, Belgium*

(Received 29 October 2018; revised manuscript received 26 January 2019; published 12 March 2019)

We report on the fabrication of conducting interfaces between $LaAlO_3$ and $SrTiO_3$ by 90° off-axis sputtering in an Ar atmosphere. At a growth pressure of 0.04 mbar the interface is metallic, with a carrier density of the order of 1×10^{13} cm^{-2} at 3 K. By increasing the growth pressure, we observe an increase of the out-of-plane lattice constants of the $LaAlO_3$ films while the in-plane lattice constants do not change. Also, the low-temperature sheet resistance increases with increasing growth pressure, leading to an insulating interface when the growth pressure reaches 0.10 mbar. We attribute the structural variations to an increase of the La/Al ratio, which also explains the transition from metallic behavior to insulating behavior of the interfaces. Our research shows that the control which is furnished by the Ar pressure makes sputtering as versatile a process as pulsed laser deposition, and emphasizes the key role of the cation stoichiometry of $LaAlO_3$ in the formation of the conducting interface.

DOI: 10.1103/PhysRevMaterials.3.034002

The discovery of a high mobility conducting interface between $LaAlO_3$ (LAO) and $SrTiO_3$ (STO) has given rise to numerous investigations [1]. This two-dimensional electron system (2DES) exhibits multiple intriguing physical properties, such as superconductivity [2], signatures of magnetism [3–6], and gate tunable insulator to metal [7] and insulator to superconductor transitions [8]. However, the origin of the 2DES in still under debate. Proposed explanations basically fall into two classes, intrinsic charge transfer and extrinsic defects mechanisms. The intrinsic mechanism considers the polar discontinuity between the polar LAO and the nonpolar STO, which leads to a charge transfer above a critical thickness of LAO films [9]. The extrinsic mechanisms involve defects formed at the interface during the film deposition process, such as oxygen vacancies in the STO substrate [10–12] and cation intermixing at the interface [13,14].

Pulsed laser deposition (PLD) is by far the most commonly used growth method to prepare LAO/STO interfaces. During the PLD process, high energy particle bombardment could introduce the above defects into the interface, which makes it difficult to understand the roles of the intrinsic and extrinsic mechanisms [14]. Other growth techniques bring new insights here. Warusawithana *et al.* [15] have grown LAO films by molecular beam epitaxy (MBE). The interesting outcome is that interfacial conductivity can be only observed in Al-rich samples (La/Al $\leqslant$ 0.97). Their further density functional theory (DFT) calculations demonstrate the different roles of defects in the charge transfer mechanism. In Al-rich samples, Al can fill La vacancies without changing the net charge of the (001) planes. The electronic reconstruction can still transfer electrons to the interface. In La-rich samples, however, La cannot substitute for Al, resulting in the formation of Al_2O_3-vacancy complexes which prohibits the charge transfer.

Sputtering also has been used. High-pressure (1 mbar) on-axis sputtering yielded LAO films with a La/Al ratio of 1.1, and insulating interfaces [16]. 90° off-axis sputtering has been shown to be capable of growing epitaxial and smooth films with conducting interfaces [17]. Sputtering is widely used in industry, which can also facilitate the device applications of LAO/STO interfaces. In this work we show the growth of high quality epitaxial LAO films by 90° off-axis sputtering. The La/Al ratio is tuned by varying the growth pressure. As a consequence, we observe strong but controlled variations in the interfacial conductivity.

LAO films were grown on TiO_2-terminated STO (001) substrates. In order to obtain the TiO_2 termination, the substrates were etched by buffered HF for 30 s and annealed at 980 °C in flowing oxygen (150 sccm) for 1 h [18]. In the sputtering chamber, the working distances were 75 mm from the surface of the heater to the axis of the target and 45 mm from the surface of the target to the axis of the heater. It should be noted that the proper choice of growth pressure is strongly dependent on the working distances. A 2-in. single crystal LAO wafer was used as the sputtering target. The growth temperature was 800 °C and the rf power was 50 W. Five samples were grown at various Ar pressures from 0.04 to 0.10 mbar (see Table I). In the following the samples will be referred to with their growth pressure (sample 004 is grown at 0.04 mbar etc.). The target was presputtered for at least 15 min in order to stabilize an oxygen background partial pressure produced by the target [17]. After deposition, the samples were *in situ* annealed in 1 mbar oxygen at 600 °C for 1 h to remove the oxygen vacancies in the STO substrates. The samples were then cooled down to room temperature in the same oxygen atmosphere at a rate of 10 °C/min. The deposition rate decreases from 4.27 Å/min at 0.04 mbar to 3.20 Å/min at 0.10 mbar. Two reference samples were prepared to test the effectiveness of the oxygen annealing treatment. One sample is a bare STO substrate heated up to the growth temperature without film deposition. The other sample is an amorphous LAO/STO sample grown at room temperature at 0.08 mbar. Both samples were highly conductive, which indicates the presence of oxygen vacancies [19–22]. The samples then underwent the above oxygen annealing treatment and were found to be insulating.

 ©2019 American Physical Society

TABLE I. Growth pressure, in-plane lattice constant (a_{LAO}), out-of-plane lattice constant (c_{LAO}), thickness (t_{LAO}), and La/Al ratio of LAO films.

Growth pressure (mbar)	a_{LAO} (Å)	c_{LAO} (Å)	t_{LAO} (u.c.)	La/Al ratio[a]
0.04	3.905(2)	3.734	16	0.88
0.06	3.905(1)	3.739	15	0.89
0.08	3.905(1)	3.745	15	0.91
0.09	3.905(2)	3.751	14	0.94
0.10	3.905(3)	3.763	17	1.00

[a]Interpolated La/Al ratios from Ref. [23].

It is noteworthy to mention two crucial issues in the film deposition process. The first issue is the selection of sputtering target. We repeated the above mentioned deposition process using a commercial sintered target (Kurt J. Lesker). The Ar pressure was tuned from 0.05 to 0.50 mbar. However, we found rough surfaces and insulating interfaces in all the samples. The second issue is the use of oxygen during deposition. We used a mixture of 2% oxygen and 98% Ar, while keeping the total pressure at 0.04 mbar. The oxygen partial pressure ($P_{O2} = 8 \times 10^{-}4$ mbar) was the lowest one that we could control. The film was deposited with other growth parameters kept constant as mentioned above and it was cooled down in the same growth atmosphere after deposition. Again, the sample was insulating with a rough surface. Therefore, samples with flat surfaces and conducting interfaces can only be obtained by using a single crystal target and depositing in a pure Ar atmosphere.

Surface topologies were measured by tapping mode atomic force microscopy (AFM). The epitaxial quality of the interface was characterized by scanning transmission electron microscopy (STEM). Film thicknesses and lattice constants were determined by high-resolution x-ray diffraction (HRXRD). Magnetotransport properties were measured with a Quantum Design physical property measurement system (PPMS) by sweeping the magnetic field between ±9 T. The measurements were performed in the van der Pauw geometry. Ohmic contacts were formed by wedge bonding Al wire directly to the sample surface.

Figures 1(a) and 1(b) show the AFM topographic images of samples 004 and 010. An atomically flat surface with clear step-and-terrace structure can be observed. The inset shows the step height which corresponds to the STO (001) interplanar distance (≈3.905 Å). The epitaxial quality of the films was further characterized by high-angle annular dark field

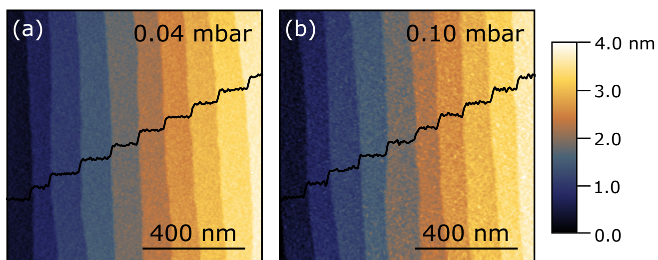

FIG. 1. AFM images of samples (a) 004 and (b) 010, using color code for the height. Insets are the height profiles of the surfaces.

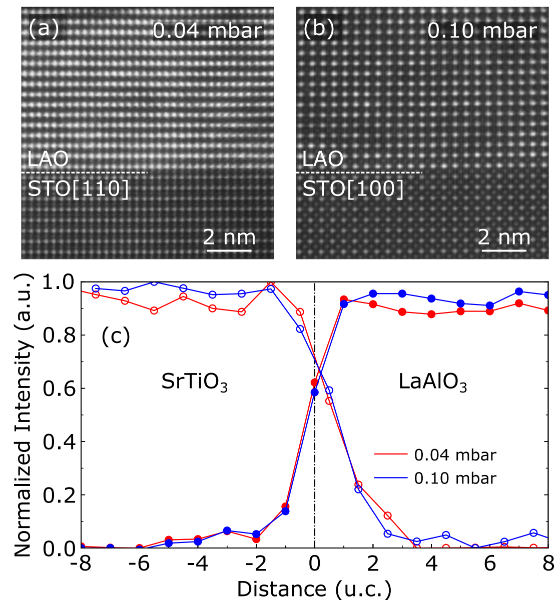

FIG. 2. High-angle annular dark field STEM (HAADF-STEM) images of (a) sample 004 taken along the [110] direction and (b) sample 010 taken along the [100] direction. (c) STEM electron energy loss spectroscopy (STEM-EELS) analysis of samples 004 and 010, the La-$M_{4,5}$ (solid circles) and Ti-$L_{2,3}$ (open circles) edges integrated unit cell by unit cell across the interface.

STEM (HAADF-STEM). As shown in Figs. 2(a) and 2(b), well ordered interfaces between the film and the substrate are clearly visible. Figure 2(c) shows the STEM electron energy loss spectroscopy (STEM-EELS) analysis of samples 004 and 010. This concentration profile is obtained by integration of the EELS intensity of the La-$M_{4,5}$ and Ti-$L_{2,3}$ edges during a spectrum image unit cell by unit cell in the growth direction. The profile is normalized by the maximum of intensity and cation vacancies are neglected. Identical intermixing (4 unit cells) was observed for both samples. This demonstrates that interdiffusion is a phenomenon that is not influenced by the growth pressure of the film.

Figures 3(a) and 3(b) show the reciprocal space maps (RSM) around the STO (103) diffraction peak of samples 004 and 010. The films are coherently strained to the substrate, which means that in-plane lattice constants (a_{LAO}) are 3.905 Å. Figure 3(c) shows the θ-2θ scans. The dashed lines are the positions of LAO (002) diffraction peaks. It can be seen that as the growth pressure increases, the LAO peak shifts to lower angle, which corresponds to an increase of the out-of-plane lattice constant (c_{LAO}) [23]. By fitting the interference fringes, we extract c_{LAO} as well as the film thickness (t_{LAO}). Table I summarizes the estimated values for a_{LAO}, c_{LAO}, and t_{LAO} of the samples. It has been reported that the increase of c_{LAO} is due to the increase of the La/Al ratio in LAO films. The relationship between them was systematically studied by Qiao *et al.* [23]. Thus we extract the La/Al ratios of our samples by interpolating our data points using their published results. The interpolated La/Al ratios are listed in Table I. As the growth pressure increases from 0.04 to 0.10 mbar, the La/Al ratio increases from 0.88 to 1.00.

Figure 4(a) shows the temperature dependence of the sheet resistance (R_s) for samples grown at various Ar pressures.

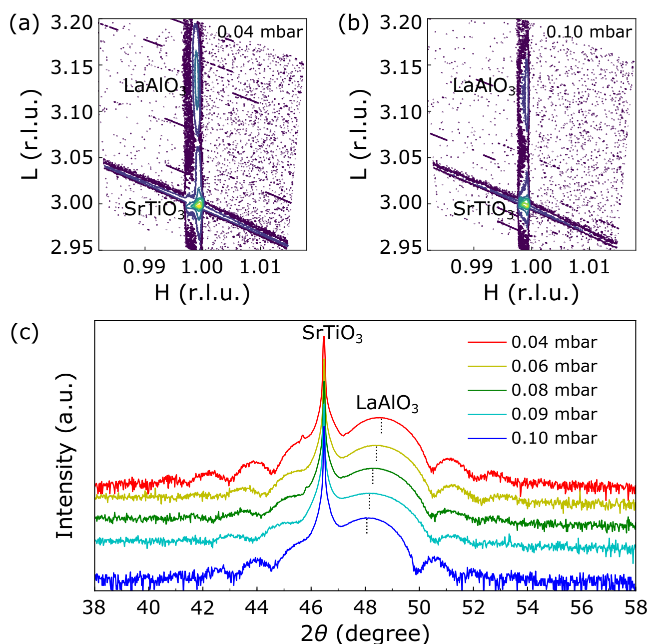

FIG. 3. Reciprocal space maps (RSM) around the STO (103) diffraction peak of samples (a) 004 and (b) 010. (c) The θ-2θ scans for samples grown at various Ar pressures. The dashed lines are the LAO (002) diffraction peaks.

Samples 004, 006, and 008 show similar metallic behavior from 300 to 3 K. The interfacial conductivity changes dramatically as the growth pressure further increases. For sample 009, R_s decreases from $1.4 \times 10^5\ \Omega/\square$ at 300 K to $1.1 \times 10^4\ \Omega/\square$ at 60 K and then gradually increases to $2.2 \times 10^5\ \Omega/\square$ at 3 K. For sample 010, R_s decreases from $3.5 \times 10^5\ \Omega/\square$ at 300 K to $1.6 \times 10^5\ \Omega/\square$ at 100 K and abruptly changes to insulating

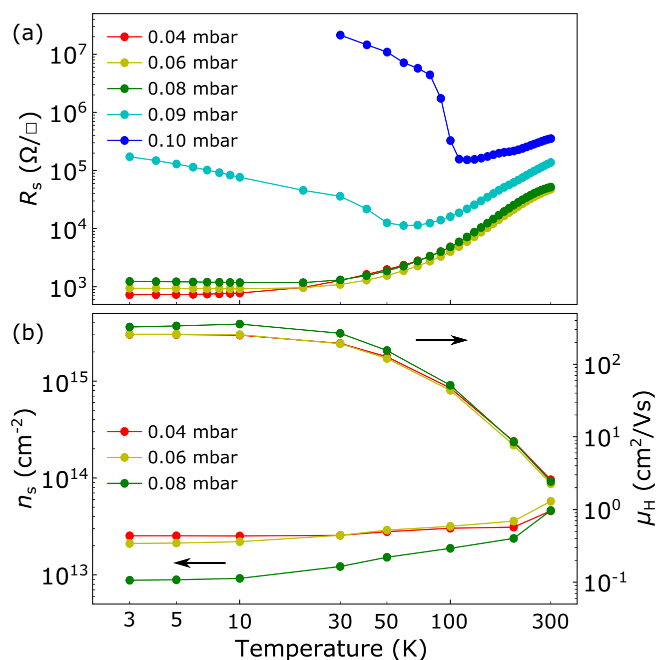

FIG. 4. Temperature dependence of (a) the sheet resistance (R_s) and (b) the carrier density (n_s) and the Hall mobility (μ_H) for samples grown at various Ar pressures.

state afterwards. The temperature dependence of the carrier density (n_s) and the Hall mobility (μ_H) for the metallic samples are shown in Fig. 4(b). n_s and μ_H were determined by $n_s = 1/eR_H$ and $\mu_H = R_H/R_s$, where e and R_H are the electron charge and the Hall coefficient, respectively. n_s and μ_H are approximately 1×10^{13} and 2.6×10^2 cm^2/Vs, respectively, at 3 K, which is consistent with reported results of LAO/STO interfaces grown by sputtering [17] and PLD [10,22].

Our observations are consistent with the results reported by Warusawithana *et al.* [15], namely that only Al-rich LAO gives rise to a conducting interface. All of our LAO films are epitaxially strained to STO substrates. Increasing the growth pressure only increases the La/Al ratio, which we believe is due to light Al being scattered more easily at higher pressures [16,24]. The dramatic change in the transport properties is related to the change of cation stoichiometry of the LAO films. For the LAO/STO samples grown by PLD, it has been also reported that a slight variation in growth parameters modifies the cation stoichiometry of LAO [24–26], resulting in a dramatic change in the interfacial conductivity. But the cation stoichiometry is not checked on a routine basis. It may explain the fact that samples from different PLD groups are often hardly comparable, although similar growth parameters are used.

Our results help to gain some insights into the origin of the 2DES. First, it is well known that La-doped STO shows metallic behavior [27]. At the LAO/STO interface, La/Sr intermixing could be induced in two ways. One way is simply by the PLD process itself, during which the STO substrate is bombarded by particles with kinetic energies around several tens of eV [14]. In our off-axis sputtering deposition, we use relatively high Ar pressures (0.04–0.10 mbar), which correspond to mean free paths of several millimeters. The direct distance between the center of the target and the substrate is about 87.5 mm. The ejected particles would undergo multiple scatterings to slow down their speed before they deposit on the substrate. In our case, the chance of introducing La/Sr intermixing by high energy particle bombarding should be low. The other way is the dipole compensation mechanism proposed by Nakagawa *et al.* [9], where a compensating dipole is produced by La/Sr intermixing to reduce the interface dipole energy. We observed identical intermixing in samples 004 and 010. However, the intermixing does not appear to be crucial to the origin of conductivity. Otherwise the two samples would show similar conducting behavior.

Next, we discuss other possible mechanisms for the interfacial conductivity. Based on DFT calculations, Warusawithana *et al.* [15] concluded that the driver of conductivity is electronic reconstruction. However, it cannot be reconciled with the experimental observation that stoichiometric LAO films grown by MBE and sputtering give rise to insulating interfaces. The fact that conductivity is only observed in Al-rich films may point to the oxygen vacancies being the doping mechanism. In this scenario, the excess Al in Al-rich films getter oxygen from the STO, which becomes n-type doped. Here we note that our samples grown in a mixture of 2% oxygen and 98% Ar show an insulating behavior. We suggest that the oxygen leads to oxidation of Al during the propagation towards the substrate [28], so that the Al is

passivated and oxygen vacancies are not formed. The limited conductivity in stoichiometric LAO films grown by PLD [24] can similarly be explained by defect generation induced by energetic particles in the ablation plume. On the other hand, we also observed that a conducting amorphous LAO/STO sample became insulating after post annealing in oxygen. This would indicate that the annealing treatment is efficient enough to remove the oxygen vacancies which are formed by the redox reaction [21]. It is therefore still not fully clear whether the observed conductivity in Al-rich samples is completely dominated by the oxygen vacancies formed in STO, but our observations on sputtered interfaces give good reasons to believe that the formation of oxygen vacancies is an important part of the puzzle.

In conclusion, high quality epitaxial LAO films were grown on STO (001) substrates by 90° off-axis sputtering. While increasing the growth pressure, little structural variations have been observed, except for an increase of the out-of-plane lattice constant, which indicates an increase of the La/Al ratio. Metallic conducting interfaces were only found in Al-rich samples. Our results emphasize that cation stoichiometry in LAO films plays an important role in the formation of interfacial conductivity at the LAO/STO interfaces.

We thank Nikita Lebedev, Aymen Ben Hamida, and Prateek Kumar for useful discussions and Giordano Mattoni, Jun Wang, Vincent Joly, and Hozanna Miro for their technical assistance. We also thank Jean-Marc Triscone and his group for sharing their design of the sputtering system with us. This work is part of the FOM research programme DESCO with Project No. 149, which is (partly) financed by the Netherlands Organisation for Scientific Research (NWO). C.Y. is supported by China Scholarship Council (CSC) with Grant No. 201508110214. N.G., D.K., and J.V. acknowledge financial support from the GOA project "Solarpaint" of the University of Antwerp.

[1] A. Ohtomo and H. Y. Hwang, Nature (London) **427**, 423 (2004).
[2] N. Reyren, S. Thiel, A. D. Caviglia, L. F. Kourkoutis, G. Hammerl, C. Richter, C. W. Schneider, T. Kopp, A.-S. Ruetschi, D. Jaccard, M. Gabay, D. A. Muller, J.-M. Triscone, and J. Mannhart, Science **317**, 1196 (2007).
[3] A. Brinkman, M. Huijben, M. V. Zalk, J. Huijben, U. Zeitler, J. C. Maan, W. G. V. D. Wiel, G. Rijnders, D. H. A. Blank, and H. Hilgenkamp, Nat. Mater. **6**, 493 (2007).
[4] L. Li, C. Richter, J. Mannhart, and R. C. Ashoori, Nat. Phys. **7**, 762 (2011).
[5] J. A. Bert, B. Kalisky, C. Bell, M. Kim, Y. Hikita, H. Y. Hwang, and K. A. Moler, Nat. Phys. **7**, 767 (2011).
[6] J.-S. Lee, Y. W. Xie, H. K. Sato, C. Bell, Y. Hikita, H. Y. Hwang, and C.-C. Kao, Nat. Mater. **12**, 703 (2013).
[7] S. Thiel, G. Hammerl, A. Schmehl, C. W. Schneider, and J. Mannhart, Science **313**, 1942 (2006).
[8] A. D. Caviglia, S. Gariglio, N. Reyren, D. Jaccard, T. Schneider, M. Gabay, S. Thiel, G. Hammerl, J. Mannhart, and J.-M. Triscone, Nature (London) **456**, 624 (2008).
[9] N. Nakagawa, H. Y. Hwang, and D. A. Muller, Nat. Mater. **5**, 204 (2006).
[10] A. Kalabukhov, R. Gunnarsson, J. Börjesson, E. Olsson, T. Claeson, and D. Winkler, Phys. Rev. B **75**, 121404(R) (2007).
[11] W. Siemons, G. Koster, H. Yamamoto, W. A. Harrison, G. Lucovsky, T. H. Geballe, D. H. A. Blank, and M. R. Beasley, Phys. Rev. Lett. **98**, 196802 (2007).
[12] G. Herranz, M. Basletić, M. Bibes, C. Carrétéro, E. Tafra, E. Jacquet, K. Bouzehouane, C. Deranlot, A. Hamzić, J.-M. Broto, A. Barthélémy, and A. Fert, Phys. Rev. Lett. **98**, 216803 (2007).
[13] P. R. Willmott, S. A. Pauli, R. Herger, C. M. Schlepütz, D. Martoccia, B. D. Patterson, B. Delley, R. Clarke, D. Kumah, C. Cionca, and Y. Yacoby, Phys. Rev. Lett. **99**, 155502 (2007).
[14] S. A. Chambers, M. H. Engelhard, V. Shutthanandan, Z. Zhu, T. C. Droubay, L. Qiao, P. V. Sushko, T. Feng, H. D. Lee, T. Gustafsson, E. Garfunkel, A. B. Shah, J.-M. Zuo, and Q. M. Ramasse, Surf. Sci. Rep. **65**, 317 (2010).
[15] M. P. Warusawithana, C. Richter, J. A. Mundy, P. Roy, J. Ludwig, S. Paetel, T. Heeg, A. A. Pawlicki, L. F. Kourkoutis, M. Zheng, M. Lee, B. Mulcahy, W. Zander, Y. Zhu, J. Schubert, J. N. Eckstein, D. A. Muller, C. S. Hellberg, J. Mannhart, and D. G. Schlom, Nat. Commun. **4**, 2351 (2013).
[16] I. M. Dildar, D. B. Boltje, M. H. S. Hesselberth, J. Aarts, Q. Xu, H. W. Zandbergen, and S. Harkema, Appl. Phys. Lett. **102**, 121601 (2013).
[17] J. P. Podkaminer, T. Hernandez, M. Huang, S. Ryu, C. W. Bark, S. H. Baek, J. C. Frederick, T. H. Kim, K. H. Cho, J. Levy, M. S. Rzchowski, and C. B. Eom, Appl. Phys. Lett. **103**, 071604 (2013).
[18] G. Koster, B. L. Kropman, G. J. H. M. Rijnders, D. H. A. Blank, and H. Rogalla, Appl. Phys. Lett. **73**, 2920 (1998).
[19] J. F. Schooley, W. R. Hosler, and M. L. Cohen, Phys. Rev. Lett. **12**, 474 (1964).
[20] C. Cancellieri, N. Reyren, S. Gariglio, A. D. Caviglia, A. Fête, and J.-M. Triscone, Europhys. Lett. **91**, 17004 (2010).
[21] Y. Chen, N. Pryds, K. J. E., G. Koster, J. Sun, E. Stamate, B. Shen, G. Rijnders, and S. Linderoth, Nano Lett. **11**, 3774 (2011).
[22] Z. Q. Liu, C. J. Li, W. M. Lü, X. H. Huang, Z. Huang, S. W. Zeng, X. P. Qiu, L. S. Huang, A. Annadi, J. S. Chen, J. M. D. Coey, T. Venkatesan, and Ariando, Phys. Rev. X **3**, 021010 (2013).
[23] L. Qiao, T. C. Droubay, T. Varga, M. E. Bowden, V. Shutthanandan, Z. Zhu, T. C. Kaspar, and S. A. Chambers, Phys. Rev. B **83**, 085408 (2011).
[24] E. Breckenfeld, N. Bronn, J. Karthik, A. R. Damodaran, S. Lee, N. Mason, and L. W. Martin, Phys. Rev. Lett. **110**, 196804 (2013).
[25] M. Golalikhani, Q. Y. Lei, G. Chen, J. E. Spanier, H. Ghassemi, C. L. Johnson, M. L. Taheri, and X. X. Xi, J. Appl. Phys. **114**, 027008 (2013).
[26] H. K. Sato, C. Bell, Y. Hikita, and H. Y. Hwang, Appl. Phys. Lett. **102**, 251602 (2013).
[27] O. A. Marina, N. L.Canfield, and J. W. Stevenson, Solid State Ionics **149**, 21 (2002).
[28] R. Groenen, J. Smit, K. Orsel, A. Vailionis, B. Bastiaens, M. Huijben, K. Boller, G. Rijnders, and G. Koster, APL Mater. **3**, 070701 (2015).